

Experimental and theoretical studies of the structure and IR spectra of neutral diamagnetic binuclear iron nitrosyl complexes

$\text{Fe}_2(\mu\text{-SC}_{6-n}\text{H}_{5-n}\text{N}_n)_2(\text{NO})_4$ ($n = 0, 1, 2$)

A. F. Shestakov,* Yu. M. Shul'ga, N. S. Emel'yanova, N. A. Sanina, and S. M. Aldoshin

Institute of Problems of Chemical Physics, Russian Academy of Sciences,
1 prosp. Akad. Semenova, 142432 Chernogolovka, Moscow Region, Russian Federation.
Fax: +7 (496) 515 5420. E-mail: a.s@icp.ac.ru

Geometric and electronic structures of the iron thiolate tetranitrosyl complexes $\text{Fe}_2(\mu\text{-SC}_{6-n}\text{H}_{5-n}\text{N}_n)_2(\text{NO})_4$, $n = 0, 1, 2$) were calculated using the B3LYP and PBE density functional methods. The geometric structures of the complexes found by the both theoretical approaches well agree with experiment, and a divergence of bond lengths is at most several hundredths of angstrom. According to the experimental data, the ground state of the system is diamagnetic, with the antiparallel orientation of the local spins 1/2 of the $\text{Fe}(\text{NO})_2$ fragments. The NO group bears a small negative charge mostly concentrated on the O atom, and the Fe—NO bond should be considered as homopolar. The formal electronic configuration of Fe is d^7 , which corresponds to the oxidation state 1+. However, in view of the presence of two homopolar bonds, the Fe atoms in the complexes should be trivalent. The both methods used well reproduce the experimental structure of the IR spectrum, but the PBE functional gives somewhat better description of the absolute position of the lines and the B3LYP functional better describes their relative intensities. The shifts of the vibrational bands of the thiolate ligand in the spectra of the complexes to both long- and short-wavelength regions are theoretically reproduced both qualitatively and semiquantitatively. Comparison of the calculated and measured splittings of the doublet of the stretching NO vibrations made it possible to attribute the appreciable disorder of splitting ($15\text{--}55\text{ cm}^{-1}$) to the structural nonequivalence of the NO groups in the complexes. Due to peculiarities of NO binding, even a small difference in the N—O and Fe—N distances ($\sim 0.01\text{ \AA}$) affects the frequency of the NO vibrations.

Key words: sulfur-containing iron nitrosyl complexes, NO donors, IR spectroscopy, density functional theory, electronic structure.

In the area of coordination chemistry increased attention is given to syntheses of metal nitrosyl complexes and studies of their electronic structure and reactivity.¹ Recently, researchers became more interested in metal nitrosyl complexes due to the discovered possibilities of their use as efficient NO donors in medicine, for instance, for controlling blood pressure^{2,3} and in photodynamic therapy.^{4,5} Binding of NO with active centers of metal enzymes, in particular, with heme and non-heme iron-containing proteins are being studied especially intensively.^{6–9} The sulfur-containing iron nitrosyl complexes are¹⁰ synthetic models of active centers of the nitrosyl [2Fe—2S] proteins, *viz.*, natural "depot" of NO. The [2Fe—2S] complexes with azaheterocyclic thiolyl groups are capable of yielding^{11,12} NO upon protonation, as well as ethers of Russen's "red salts" $\text{Fe}_2(\text{SR})_2(\text{NO})_4$ ($\text{R} = \text{Et}$,¹³ Bu^t ,^{14,15} $(\text{CH}_2)_4\text{—Me}$,¹⁴ $\text{C}_6\text{H}_4\text{F}$,¹⁶ Ph ¹⁷). The latter, as known, generate NO in the light and can serve as the basis for preparation of medicines.

In our previous works,^{18,19} we described the synthesis and studied the structures of the related diamagnetic complexes $\text{Fe}_2(\mu\text{-SC}_{6-n}\text{H}_{5-n}\text{N}_n)_2(\text{NO})_4$ ($n = 1, 2$) with biologically active azaheterocyclic ligands, *viz.*, analogs of nucleic acid components used as antumor agents in the cancer therapy. It seems of certain interest to interpret IR spectra of these compounds. We have earlier²⁰ advanced a hypothesis about structural nonequivalence of the NO groups in the sulfur-containing binuclear nitrosyl complexes of the $\mu\text{-S}$ and $\mu\text{-N—C—S}$ types.

In the present work, we performed the quantum chemical study of the electronic structures of the complexes with simultaneous simulation of the IR spectra and compared them with experiment. To extent the series of related complexes, we considered the complex with the $\text{Fe}_2(\mu_2\text{-SPh})_2(\text{NO})_4$ thiophenol bridge, whose synthesis is described¹⁷ but X-ray diffraction data are lacking.

Electronic structure of the complexes

The structures, electronic structures, and properties of the binuclear iron dinitrosyl complexes $\text{Fe}_2(\mu\text{-SR})_2(\text{NO})_4$ ($\text{R} = \text{Ph}$ (**1**), $\text{C}_5\text{H}_4\text{N}$ (**2**), $\text{C}_4\text{H}_3\text{N}_2$ (**3**)) were studied by the B3LYP and PBE density functional methods. In the first case, the 6-31G* and 6-311++G** basis sets were used for geometry optimization and calculation of the energy of the optimized structures, respectively, as well as the GAUSSIAN-98 program.²¹ In the second case, the Fe [5s5p4d] C, N, O, S [3s3p2d], and H [3s1p] extended basis sets for the SBK pseudo potential and the PRIRODA program were used.²² The calculated and experimental geometric parameters of the complexes are presented in Fig. 1. As a whole, the difference between the theory and experiment does not exceed several hundredths of angstrom for bond lengths and 1–2° for angles, except for the Fe–Fe distances, which are systematically underestimated by 0.17 and 0.06 Å in the B3LYP and PBE approaches, respectively. According to the calculation, the isolated molecules have the C_{2h} symmetry and, therefore, all the NO groups are equivalent. However, packing effects result in their nonequivalence. For instance, in the complex with $n = 1$ the short intermolecular contact between the O atoms of the NO ligands and the H atoms of the pyridine ring elongates the N–O bond and shortens the Fe–N bond by 0.06 and 0.02 Å, respectively. The symmetry of complex **1** is least distorted.

The bridging ligand in the neutral binuclear $\text{Fe}_2(\text{SR})_2(\text{NO})_4$ complexes can be considered as the negatively charged SR^- group. Thus, an odd number of electrons falls on each Fe center and, hence, its spin is non-zero. For the short Fe–Fe distances ~ 2.7 Å as in complexes **1–3**, the spin-paired diamagnetic state of the system is observed. This singlet state can most adequately be reproduced only using the multideterminant wave function including the superposition of electronic configurations corresponding to two possible manners of mutual orientation of the localized spins $\text{Fe}\uparrow\text{Fe}\downarrow$ and $\text{Fe}\downarrow\text{Fe}\uparrow$. The calculation shows that triplet instability of the solution appears for the description of the singlet state in the framework of the one-determinant approach when electrons with opposite spins occupy the same MO. In fact, in the B3LYP/6-31G* approach, the triplet states of complexes **1**, **2**, and **3** are lower in energy than the singlet states by 5.8, 8.8, and 7.0 kcal mol⁻¹, respectively. The electronic structure can approximately be described on going to the one-determinant wave function with broken symmetry and non-zero and oppositely oriented spins on the Fe atoms. This function simulates the true multideterminant wave function for the singlet state of a system with open shells. In this approximation, the energy of the system is lower by 18.8, 20.4, and 19.5 kcal mol⁻¹, respectively. Therefore, the true multideterminant singlet state is still lower in energy due to the contribution of the

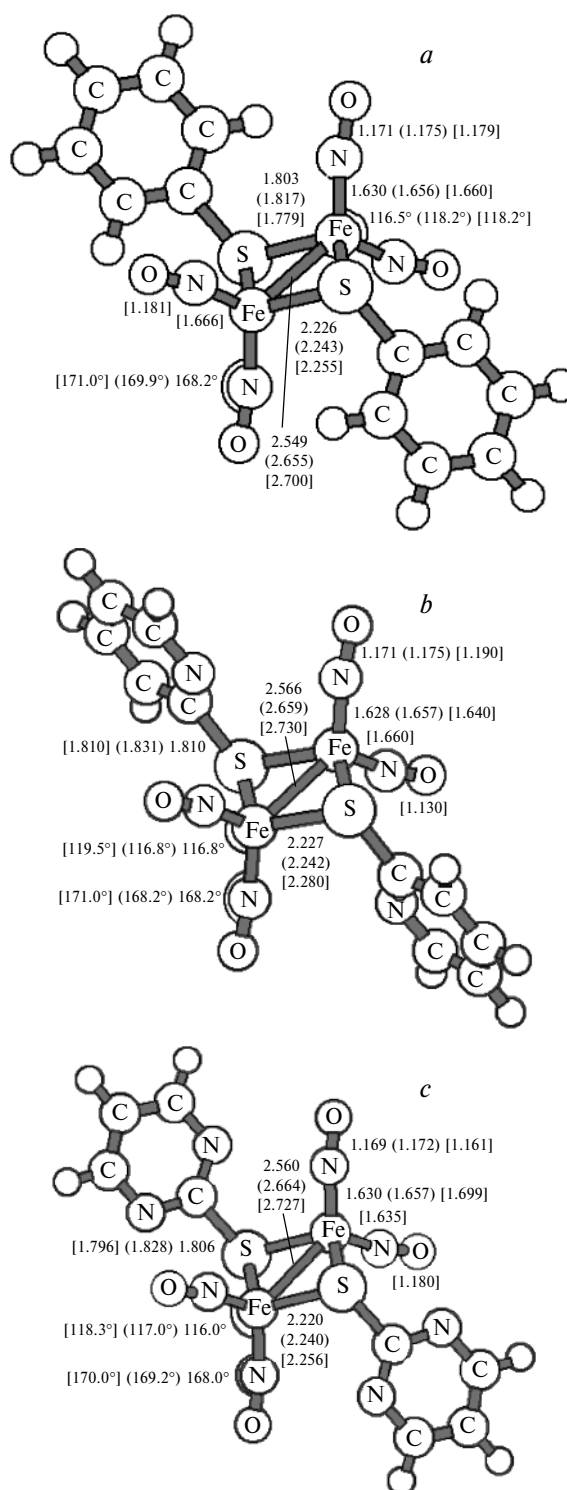


Fig. 1. Structures of the $\text{Fe}_2(\mu\text{-SPh})_2(\text{NO})_4$ (**1**) (a), $\text{Fe}_2(\mu\text{-SC}_5\text{H}_4\text{N})_2(\text{NO})_4$ (**2**) (b), and $\text{Fe}_2(\mu\text{-SC}_4\text{H}_3\text{N}_2)_2(\text{NO})_4$ (**3**) (c) complexes; interatomic distances (Å) and angles (deg) are indicated; experimental values are given in brackets (a)*, (b)¹⁸, and (c)¹⁹, and the values calculated by the PBE method are presented in parentheses.

* A. N. Chekhlov and S. M. Aldoshin, unpublished results.

energy of resonance of configurations with different types of spin localization. However, when calculating in the extended 6-311++G** basis set even without this correction, the energy of the singlet state of complexes **1**, **2**, and **3** is lower than the triplet state energy by 16.0, 14.3, and 15.4 kcal mol⁻¹, respectively. Thus, the B3LYP calculation gives the diamagnetic ground state of the complexes, which agrees with the experimental data.

The charges and spin densities on atoms for the symmetric and nonsymmetric singlet states of the complexes are given in Table 1. It can be seen that each Fe(NO)₂ unit contains one unpaired electron. However, this state occurs when the spin 3/2 of the Fe atom is bound with the oppositely oriented spins *S* = 1/2 of two NO groups. Thus, in the simplest approach, the wave function of the Fe₂(μ₂-SR)₂(NO)₄ complexes can be considered as the superposition of two configurations Fe↑↑↑NO↓NO↓Fe↓↓↓NO↑NO↑ and Fe↓↓↓NO↑NO↑Fe↑↑↑NO↓NO↓. For the singlet state with broken symmetry in an H₂ molecule, similar distribution of the oppositely oriented spins 1/2 by the H atoms appears. This pattern corresponds to the homopolar H—H bond for H₂ and homopolar Fe—NO bonds for the nitrosyl complexes. Thus, the chemical bonds of the Fe atom with its ligand environment are mixed. First, it is oxidized (due to one electron donation to the SR group); second, two covalent bonds with the NO molecules are formed, *i.e.*, effective valency of the Fe atom can be de-

termined as 3. Since no substantial electron density redistribution occurs between the Fe atoms and NO groups, the formal electronic configuration of the Fe atom remains to be d⁷ (as for Fe⁺). The formal valency 3 is consistent with resistance of the crystalline complexes to oxidation with air, and the electronic configuration d⁷ corresponds to the NGR data.¹⁰ The calculated Mulliken charges on the NO group are small and negative (from -0.21 to -0.25), and their values calculated by the B3LYP and PBE methods almost coincide. The small shift of the NO vibration frequency for complex formation compared to its change on going from NO to NO⁻ confirms a small charge on the nitrosyl group. The sign of the charge and the decrease in the frequency of NO vibrations indicate the acceptor properties of the NO group. However, the virtually linear coordination of the NO ligands indicates that the accepted electron density is not high enough for nonlinear coordination of the NO groups corresponding to the substitution of the H atom for metal in the nonlinear HNO molecule to occur.

As can be seen from the data in Table 1, the triplet state of the nitrosyl complexes can be accomplished by several procedures. For instance, for complexes **2** and **3** we were able to localize the triplet state, whose energy is higher than those of the singlet state with closed shells by 29.0 and 21.3 kcal mol⁻¹, respectively. It follows from the data for the average squared spin (see Table 1) that the excited state for complex **2** is one-configurational and

Table 1. Electronic characteristics of the Fe₂(μ-SC_{6-n}H_{5-n}N_n)₂(NO)₄ complexes (*n* = 0, 1, 2)

Complex	Δ <i>E</i> /kcal mol ⁻¹	Multiplicity	Fe		NO		⟨ <i>S</i> ² ⟩	⟨ <i>S</i> ² ⟩ ^a
			Charge	Spin density	Charge	Spin density		
Calculation by B3LYP/6-31G*								
1	-21.0	1 ^b	0.62	±2.41	-0.23	±0.77	2.62	10.82
	-5.8	3	0.65	2.50	-0.22	-0.84	3.85	6.15
	0	1	0.51	—	-0.21	—	—	—
2	-20.4	1 ^b	0.63	±2.43	-0.22	±0.86	2.65	10.89
	-8.8	3	0.66	2.5	-0.21	-0.84	3.83	6.06
	0	3	0.52	—	-0.21	—	—	—
3	29.0	3	0.54	0.42	-0.17	0.24	2.08	2.00
	-31.0	1 ^b	0.61	±2.41	-0.21	±0.85	2.60	10.72
	-7.0	3	0.63	2.49	-0.21	-0.83	3.83	6.05
	0	1	0.50	—	-0.20	—	—	—
21.3	3	0.56	1.36	-0.16	-0.20	3.33	3.86	
Calculation by PBE/SBK								
1	0	1	0.50	—	-0.23	—	—	—
	18.5	3	0.64	1.80	-0.25	-0.47	—	—
2	0	1	0.49	—	-0.22	—	—	—
	16.7	3	0.63	1.78	-0.23	-0.46	—	—
3	0	1	0.50	—	-0.21	—	—	—
	16.3	3	0.66	1.84	-0.23	-0.48	—	—

^a The average value of the squared spin after annihilation of the wave function component with the spin 1 and 2 for a singlet and triplet, respectively.

^b The state with broken symmetry.

each Fe atom contains one unpaired electron. The spin density is distributed approximately by 50% between the Fe atoms and two NO ligands, which shows that the d-orbital occupied by an unpaired electron has no predominant localization on either metal or ligand. This character of MO is possible when it is formed from orbitals of the metal center and NO ligand with close energy characteristics. The remaining two electrons on the Fe atom and one electron on each NO group, which had oppositely oriented spins in the ground state configuration, now occupy two delocalized bonding MOs of the Fe–NO fragment. As a result, ionic states like $\text{Fe}^{3+}(\text{NO}^-)_2$ and $\text{Fe}^-(\text{NO}^+)_2$ types contribute noticeably to the wave function, which increases, most likely, the energy of this electron state. The energy of the singlet state with closed shells increases for the same reason.

The triplet state, whose energy is higher by $21.3 \text{ kcal mol}^{-1}$ than that of the singlet state with closed shells in complex **3**, is not already one-configurational, which follows from the value of the average squared spin. The spin density distribution indicates two unpaired electrons on the Fe atoms and one oppositely oriented unpaired electron on each of the two NO ligands. The spin density values differ from theoretical values of 2 and 0.5 due to effects of the delocalized character of MOs. If they are accepted (for estimation) the same as those for the above considered triplet state of complex **2**, we obtain the structure of spin density distribution (Fe, $0.94 + 0.42$; NO, $-0.44 + 0.24$) that explicitly indicates the presence of two unpaired electrons on the Fe atom. Compared to the triplet state for complex **2**, electrons that earlier occupied one of the bonding MOs become unpaired. Ignoring the effects of electron shell overlapping, this MO has the form

$$\varphi = 1/\sqrt{2}d + 0.5(\pi_1 + \pi_2),$$

where d and π are orbitals localized on the Fe atom and NO groups, respectively. During this unpairing, in the electronic configuration of the complex $\varphi\alpha\varphi\beta$ is replaced by $d\alpha(\pi_1 + \pi_2)/\sqrt{2}\beta$.

The new electronic configuration $\text{Fe}\uparrow\uparrow(\text{NO})_2\downarrow$ becomes closer to the true $\text{Fe}\uparrow\uparrow\uparrow(\text{NO}\downarrow\text{NO}\downarrow)$ configuration and, hence, the energy of this triplet state in complex **3** is lower than that in complex **2**: $21.3 \text{ kcal mol}^{-1}$ versus $29.0 \text{ kcal mol}^{-1}$. The spin density distribution obtained by the PBE method using the PRIRODA program indicates that in all the complexes the Fe atom contains two unpaired electrons. That is why these spin states are higher in energy than the singlet states with closed shells. Unfortunately, explicit facilities for controlling the initial approximation to the solution vector are unavailable in the PRIRODA program and, therefore, low-energy triplet states were not localized.

Comparison of the charge and spin density distributions for the singlet state with broken symmetry and the

low triplet state for complex **3** shows that they virtually coincide in absolute value. This additionally indicates the homopolar character of the Fe–NO bond that occurs without noticeable electron density migration between the metal and ligands.

IR spectroscopy

The experimental and theoretical spectra of complex **1** with the bridging thiophenol ligand and of the PhSH ligand in the region below 2000 cm^{-1} are presented in Fig. 2. The fixed Lorentz spreading of all lines with a half-width of 2 cm^{-1} was used when constructing the theoretical spectra. The strongest distinction in the theoretical spectra of the complex and ligand is the appearance of very intense lines in the region of 1800 cm^{-1} caused by stretching vibrations of the NO groups. The deconvolution

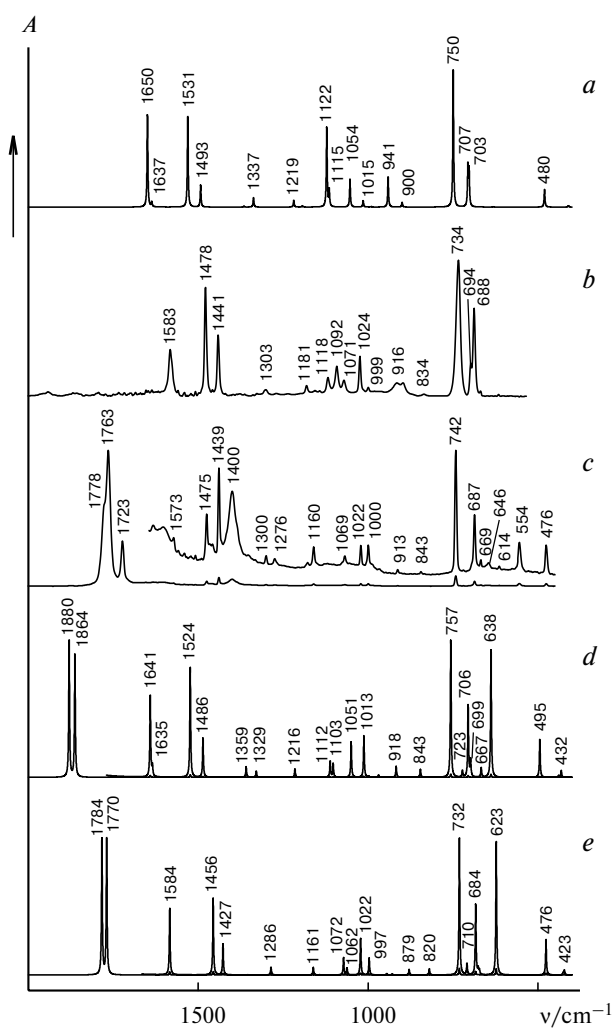


Fig. 2. IR spectra of the PhSH ligand (*a*, *b*) and $\text{Fe}_2(\mu\text{-SPh})_2(\text{NO})_4$ complex (**1**) (*c*–*e*): experiment minus the background (*a*, *c*) and calculation by the B3LYP (*b*, *d*) and PBE (*e*) methods.

of the double peak in the experimental spectrum gives two lines at 1778 and 1763 cm^{-1} with half-widths of 14 and 12 cm^{-1} , respectively, and an intensity ratio of 109 : 166. The obtained splitting (15 cm^{-1}) agrees well with the results of B3LYP (17 cm^{-1}) and PBE (16 cm^{-1}) calculations, but these calculations give approximately the same ratio of the line intensities. With account for the difference in line half-widths, the theory satisfactorily reproduces the relative differences in vibrational intensities of NO and other groups. In the B3LYP/6-31G* approximation, the vibrational frequency of the NO molecule is 1991 cm^{-1} , which exceeds the experimental value by 87 cm^{-1} . Approximately the same difference (100–102 cm^{-1}) is observed between the experimental and theoretical frequencies of NO vibrations in the complex. Quantitative discrepancy of line positions in the experimental spectra is lower, on the average, for the PBE calculation as well. However, in this case, the description of the line intensity is worse than that obtained using the B3LYP method. The results of calculations using the both methods shows that the intensity of stretching N—O vibrations in coordinated nitrogen oxide is by an order of magnitude higher than that in the free NO molecule.

The experimental spectrum (see Fig. 2, c) contains a satellite at 1723 cm^{-1} near the main double line, whose intensity is by 7 times lower. Its half-width is 8.9 cm^{-1} . The theoretical spectra (see Fig. 2, d, e) contain no additional line as in the experimental spectra of complexes **2** and **3** containing only doublets of NO vibrations.^{1,2} Since the experimental spectra of the complex and ligand in the region below 1700 cm^{-1} are well consistent, it can be assumed that this line appears due to the decomposition of the initial binuclear complex to two mononuclear complexes (with coordination of the additional ligand instead of the second bridging SPh group) during sample preparation for IR measurements. However, the ratio of intensities of the main and satellite lines is approximately constant for the complexes prepared by different methods. Therefore, the additional line appears, most likely, for another reason.

The high-frequency band at 1880 cm^{-1} is related to the inphase NO vibrations at one Fe center, and the band at 1864 cm^{-1} is assigned to NO vibrations in the antiphase. The effective mass for these vibrations is almost the same (14.70) and close to the value (14.87) for an isolated NO molecule. This indicates predominant localization of vibrations on the NO fragments, and the decrease in the vibration frequency is caused by a decrease in the force constant of the N—O bond for NO coordination. The reason is the appearance of a small negative charge on the NO group (see Table 1) and, thus, loosening of the N—O bond. It can be assumed that the degree of charge transfer to the NO group depends on the N—O distance, *i.e.*, on the phase of the NO vibration, because the position of the antibonding π -orbital of NO mixing with the

d-orbital of Fe is sensitive to the value of this distance. Therefore, for the antiphase vibration one of the NO ligands bears a more positive charge than that in equilibrium and another NO ligand is more negative. In this situation we can accept that the charge on the Fe atom would substantially remain unchanged. As a result, the effective attraction of the NO ligands appears during an antiphase vibration, resulting in a decrease in the force constant. For the inphase vibration, correlation in a change in the charges of NO results in the appearance of an additional effective repulsion between the NO groups and effective attraction between the NO ligands and Fe center. In the first approximation, these contributions would quench each other and the force constant would remain unchanged. In our opinion, this explains the character of splitting of the NO vibrations in complex **1**. In the experimental structure of complex **1** with the C_i symmetry, differences in coordination of the nonequivalent NO groups are very insignificant (see Fig. 1, a) compared to more substantial differences for complexes **2** and **3**. Therefore, the nonequivalent NO groups more strongly differ in force constants, resulting in a higher splitting of the NO vibrations (to 50 cm^{-1}), while for the theoretical spectra of the binuclear complexes with symmetric structure this splitting does not exceed 20 cm^{-1} .

It follows from a comparison of the spectra of the ligand and complex (see Fig. 2, c, d) that the main bands of the ligand are retained in the spectrum of the complex and gain small shifts, as a rule, to the long-wavelength region, but in some cases to the short-wavelength region. Comparison of the theoretical and experimental spectra shows (see Fig. 2) that, despite the difference in absolute positions of the lines, the sign and value of the calculated shift coincide satisfactorily with the measured values. Features in the spectra of the complex in the region below 1700 cm^{-1} are associated with the disappearance of the doublet at 916 cm^{-1} and the appearance of only one band instead of the triplet with the center at 1092 cm^{-1} . Moreover, additional bands appear: a broad band at 1400 cm^{-1} and several new bands with frequencies below 687 cm^{-1} , namely, at 669, 646, 614, 554, and 476 cm^{-1} . The band at 1400 cm^{-1} is an artifact. It is much broader than other bands in the spectrum, and its relative peak intensity depends on the method of sample preparation. As shown by analysis, this band is caused by NH_4Cl admixtures in KBr, which is also indicated by the second broad band (3139 cm^{-1}) characteristic of NH_4Cl . Other new bands in the theoretical spectrum (see Fig. 2, d) are related to the inphase (638 cm^{-1}) and antiphase (432 cm^{-1}) Fe—NO bending vibrations (perpendicular to the N—Fe—N plane). Large splitting of these frequencies is caused by a complicated character of the shape of vibrations with a noticeable contribution of changes in the Fe—S distances. This is indicated by a high difference in effective masses in amu ($m = 17.5$ and 12.6, respectively) and force con-

stants in $\text{mdyne } \text{\AA}^{-1}$ ($F = 4.19$ and 1.39 , respectively). An analogous situation is observed for the antiphase (723 cm^{-1} , $m = 19$, $F = 5.93$) and inphase (667 cm^{-1} , $m = 18.1$, $F = 4.75$) Fe—N stretching vibrations also mixed with the Fe—S vibrations. Based on the calculated splittings, we assign the bands at 669 and 614 cm^{-1} to the Fe—N vibrations, and the bands at 646 and 476 cm^{-1} can be ascribed to the Fe—N—O bending vibrations. Then the experimental and theoretical intensities of the Fe—N stretching vibrations approximately coincide, and for the Fe—NO bending vibrations the distribution of intensities of the low- and high-frequency lines is opposite.

The split band at 916 cm^{-1} in the spectrum of the ligand can be related to the theoretical vibration 941 cm^{-1} , which is the C—S—H bending vibration, and the splitting can be explained by the formation of hydrogen bonds between two thiophenol molecules due to which the H atoms become nonequivalent. Simultaneously one can expect the splitting of the C—S vibration in this complex, which results, in our opinion, in the appearance of two vibrations (1118 and 1092 cm^{-1}) instead of one C—S vibration (1122 cm^{-1}) in the theoretical spectrum of the PhSH monomer. These vibrations of the ligand experience the maximum shift (from 1122 to 1103 cm^{-1}) during complex formation. Therefore, we assign the band at 1069 cm^{-1} in the experimental spectrum to the C—S vibration.

The group of intense high-frequency bands of the ligand is associated with the C—C vibrations of the ring: the inphase and antiphase vibrations C(2)—C(3), C(5)—C(6) at 1650 (1583) and 1493 (1441) cm^{-1} , respectively; antiphase vibration C(1)—C(6), C(3)—C(4) at 1637 (1583) cm^{-1} ; inphase vibration C(1)—C(2), C(4)—C(5) at 1531 (1478) cm^{-1} . (Hereinafter the assigned experimental bands are given in parentheses.) In the theoretical spectrum, the bands at 1641 (1573), 1436 (1439) and 1635 (1513), 1524 (1475) cm^{-1} correspond to the above bonds. In the low-frequency region of the spectrum of PhSH, the most intense vibrations are the following: in-plane C—C—H bending vibrations of the fan type when all H atoms move the one direction perpendicularly to the aromatic ring plane — 734 (750) cm^{-1} , planar C—C—C stretching vibrations of the cycle with synchronous measurement of the C(2)—C(1)—C(6) and C(3)—C(4)—C(5) angles — 707 (698) cm^{-1} , and nonplanar bending vibrations of the cycle when the triple of atoms C(2)—C(4)—C(6) move perpendicularly to the cycle — 703 (688) cm^{-1} . The corresponding vibrations of the complex have the frequencies 757 (742), 706 (687), and 699 (687) cm^{-1} .

The less intense bands in the spectrum of the ligand belong to the C—C vibrations of the ring at 1365 (?) cm^{-1} , C—C—C bending vibrations of the ring at 1054 (1024) and 1015 (985) cm^{-1} , and C—C—H bending vibrations at 1338 (1307), 1219 (1181) 1115 (1071), 900 (?), and

843 (?) cm^{-1} . The vibrations at 1365 and 843 cm^{-1} have very low theoretical intensity and, hence, they cannot virtually be detected and the vibration at 900 cm^{-1} is blended, most likely, by a broad band at 916 cm^{-1} . The corresponding vibrations of the complex have frequencies of 1359 (1300), 1051 (1022), 1013 (1000), 1329 (1276), 1216 (1160), 1112 (1069 ?), 918 (913), and 846 (843) cm^{-1} . An analog of the vibration at 1112 cm^{-1} in the experimental spectrum is lower-intensity and unnoticeable or blended by the vibration at 1069 cm^{-1} .

For complexes **2** and **3** with the heterocyclic bridging ligand, the free RSH ligand can exist in two isomeric forms: thione and thiol. According to calculations, they have close energies and, therefore, their coexistence can be expected. As a result, unlike complex **1**, direct comparison of the experimental spectra of complexes **2** and **3** with the spectra of the corresponding ligands is poorly informative. Comparison of the theoretical spectra (Fig. 3)

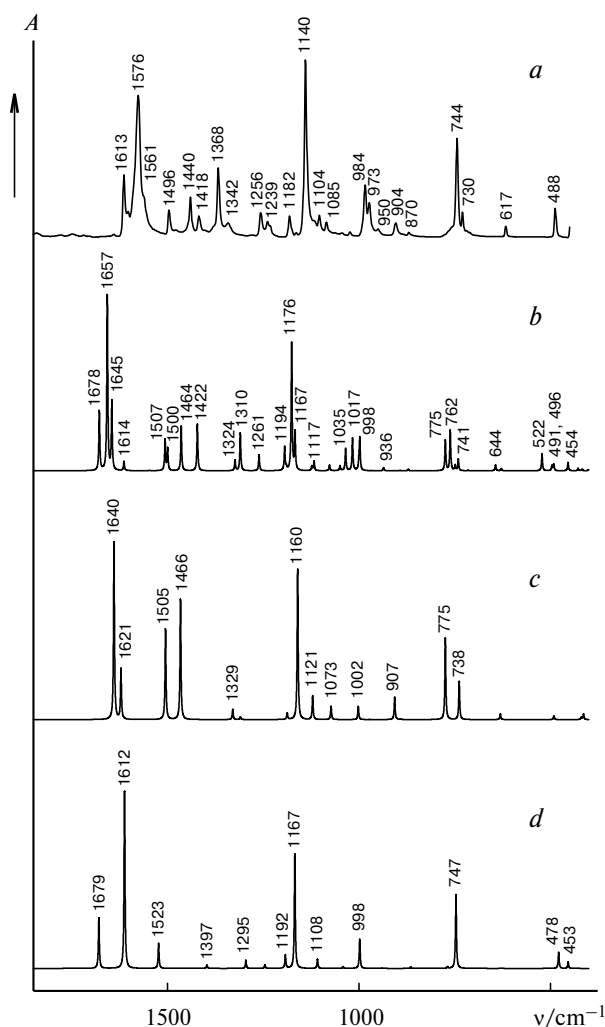


Fig. 3. IR spectra of the $\text{HSC}_5\text{H}_4\text{N}$ ligand: experiment minus the background (*a*) and calculation by the B3LYP method (*b*–*d*) for the ligand in the form of the dimer (*b*) and in the monomeric thiol (*c*) and monomeric thione (*d*) forms.

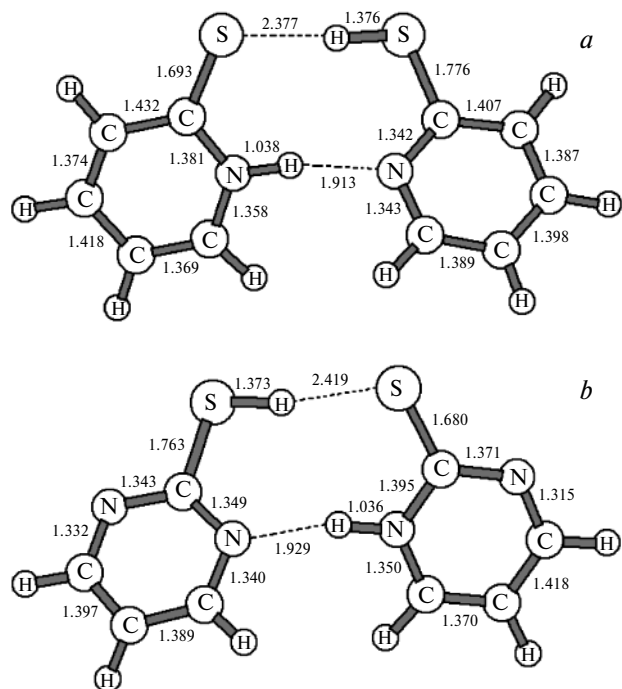


Fig. 4. Structures of the $(\text{HSC}_5\text{H}_4\text{N})_2$ (*a*) and $(\text{HSC}_4\text{H}_3\text{N})_2$ (*b*) dimers; interatomic distances (Å) and angles (deg) are indicated.

of the HSC_5NH_4 ligand in the thione (*d*) and thiol (*e*) forms with the experimental spectrum of the crystalline sample (*a*) shows their explicit discrepancy. Since information on the crystal structure of HSC_5NH_4 is lacking, the theoretical spectrum of the dimer (*b*) of the H-bonded thione and thiol forms (Fig. 4, *a*) was used for comparison as a reasonable compromise. According to the data on the B3LYP/6-311++G** calculation, the energy gain for dimer formation is even higher than the difference in the energies of thione (the main form) and thiol. The same situation is observed for the HSC_5NH_4 dimer as well (Fig. 4, *b*).

Spectra *a* and *b* (see Fig. 3) are similar in structure for both the frequency distribution of the lines and their relative intensity. At the same time, the spectrum of the dimer differs from a simple superposition of the spectra of thione and thiol. The most intense lines in the spectrum of thiol at 1640 and 1160 cm^{-1} correspond to symmetric vibrations C—C, C(1)—C(2), and C(4)—C(5) in the phase ($m = 5.08$) and planar bending vibrations C—C—H ($m = 2.78$) in which the H atoms bonded to the C(3), C(4), and C(5) atoms are mostly involved. The least intense vibrations at 1505 ($m = 2.06$), 1466 ($m = 2.05$) and 775 cm^{-1} ($m = 1.34$) are related, correspondingly, to planar bending vibrations H—C(2), H—C(5) in the antiphase and H(C(3)), H(C(4)) in the phase and inphase out-of-plane bending vibrations H—C—C in which all H atoms participate. In the theoretical spectrum of the

dimer, the above indicated five vibrations appear with the maximum frequency shifts at 1645, 1176, 1507, 1464, and 775 cm^{-1} . Their relative intensity is also approximately retained. Since the absolute intensity of the main vibrations in the spectrum of thione is by ~ 3 times higher than that in the spectrum of thiol, the thiol vibrations are minor in the spectrum of the dimer. These vibrations were assigned to the bands at 1556 (sh), 1496, 1440, 1104, and 730 cm^{-1} in the experimental spectrum.

The most intense band in the spectrum of thione at 1612 cm^{-1} ($m = 3.09$) belongs to the planar H—N—C bending vibration. The less intense bands at 1679 cm^{-1} ($m = 5.08$), 1167 cm^{-1} ($m = 2.45$), and 747 cm^{-1} ($m = 1.20$) are inphase bending vibrations of the C(1)—C(2) and C(4)—C(5) bonds, planar bending vibrations H—(N)C, H—C(2), and H(C(4)), and synchronous out-of-plane bending vibrations H—C—C and H—N—C involving all H atoms, respectively. In the spectrum of the dimer these vibrations appear at 1678, 1657, 1176, and 761 cm^{-1} . The higher the component of the N—H vibration in the total shape of vibration, the higher the absolute shift value, which is due to the involvement of this H atom in the weak hydrogen bond H...N (1.913 Å). The bands at 1613, 1576, 1140, and 744 cm^{-1} in the experimental spectrum we assign to the above vibrations. This assignment agrees with the broadened character of the band at 1576 cm^{-1} because of the labile structure of complexes with hydrogen bond.

New bands at 1422, 1035, and 1017 cm^{-1} appear due to the intensity redistribution in the spectrum of the dimer (upon dimer formation the absolute intensity of the bending H—N—C vibration decreases by 20%). This theoretical result agrees well with the presence of rather intense bands at 1368, 984, and 973 cm^{-1} in the experimental spectrum.

The experimental spectrum of complex **2** (Fig. 5, *a*) is well reproducible by calculations (Fig. 5, *b, c*); the B3LYP approach better reproduces the line intensity, and the PBE approach better reproduces the line positions. Comparison of the spectra of the ligand (see Fig. 3, *c*) and complex **2** (see Fig. 5) shows that all vibrations of the ligand in the thiol form with some shifts and slightly changed intensities are observed in the frequency region >730 cm^{-1} . New vibrations associated to the NO ligand appear in the frequency region ≤ 730 cm^{-1} in the theoretical spectrum of complex **2**. These are the symmetric (669 cm^{-1} , $m = 7.4$) and antisymmetric (722 cm^{-1} , $m = 5.6$) Fe—N stretching vibrations (with an admixture of the Fe—S vibration) and the bending vibration (640 cm^{-1} , $m = 17$). Taking into account the assignment of vibrations of this type for complex **1**, we ascribe the bands at 734 and 621 cm^{-1} in the experimental spectrum to the Fe—N stretching vibrations, and the band at 716 cm^{-1} can be assigned to the F—NO bending vibration. The stronger splitting of the Fe—N vibrations is due,

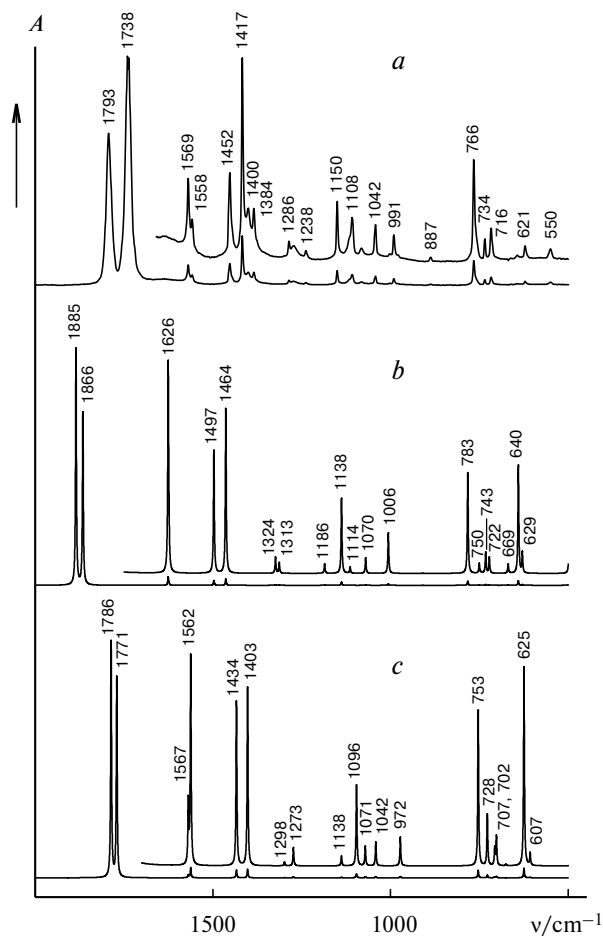


Fig. 5. IR spectra of the $\text{Fe}_2(\mu\text{-SC}_5\text{H}_4\text{N})_2(\text{NO})_4$ complex (**2**): experiment minus the background (*a*) and calculation by the B3LYP (*b*) and PBE (*c*) methods.

most likely, to the more pronounced nonequivalence of the NO groups in the crystal structure of complex **2**.

As for complex **1**, we attribute the band at 1400 cm^{-1} to an NH_4Cl admixture in the sample. However, the rather intense band at 1384 cm^{-1} has no analogs in the theoretical spectra. The region of $1464\text{--}1324\text{ cm}^{-1}$ in the spectrum of complex **2** contains no lines to which this band can be assigned if the mechanism of enhancement of its intensity would appear. The reason for the appearance of this band, as well as the band at 1723 cm^{-1} , in the spectrum of complex **1** remains unclear.

The experimental IR spectrum of crystalline mercaptopyrimidine (Fig. 6, *a*) also contains more bands than the theoretical spectra of the ligands in the form of thione (Fig. 6, *d*) or thiol (Fig. 6, *c*) and agrees satisfactorily with the spectrum of the dimer consisting of thione and thiol. As for crystalline mercaptopyridine, spectrum *b* is not a simple superposition of spectra *c* and *d* and new bands appear in it. The most intense bands at 1641 (1609), 1438 (1335), and 1239 (1190) cm^{-1} are related to the H—N—C bending vibrations, planar symmetric bending

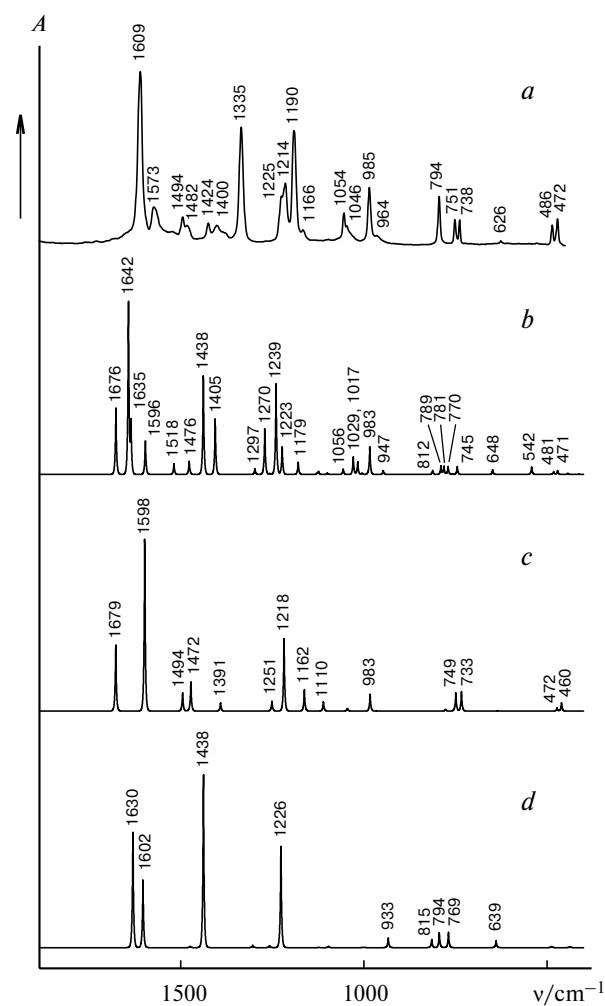


Fig. 6. IR spectra of the $\text{HSC}_4\text{H}_3\text{N}_2$ ligand: experiment minus the background (*a*) and calculation by the B3LYP method (*b*–*d*) for the ligand in the form of the dimer (*b*) and in the monomeric thiol (*c*) and monomeric thione (*d*) forms.

vibrations of the H(C(3)) and H(C(5)) atoms of thiol, and C=S stretching vibrations of thione, respectively.

Quite satisfactory agreement of the IR spectra of crystalline 2-mercaptopyridine and 2-mercaptopyrimidine with the theoretical spectra for the model dimeric structures (see Fig. 4) indicates that the crystal contains unambiguously the both isomeric forms of the ligand: thione and thiol. This fact can be significant for synthesis of the iron nitrosyl complexes, because the structures containing simultaneously the thione and thiol forms of the heterocyclic ligand with the mercapto group are known.²³

Complex **3** (Fig. 7) also exhibits good consistence of the experimental spectrum (*a*) and theoretical spectra (*b* and *c*). The structure of the spectrum is noticeably simplified due to a decrease in the number of H atoms in the ligand and its symmetric character. The most intense vibrations, excluding NO vibrations, at 1619 (1551), 1431 (1376), and 1197 (1151) cm^{-1} , correspond to the

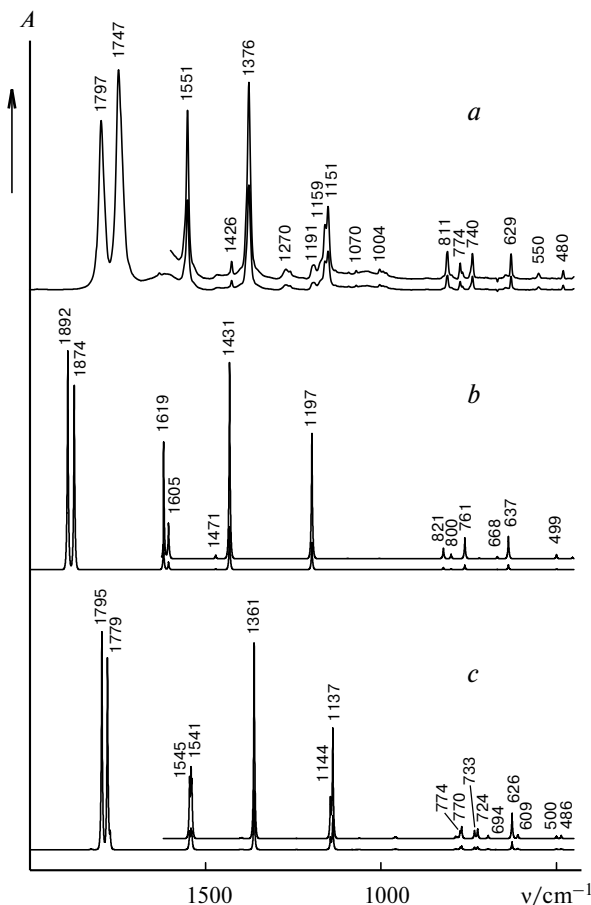


Fig. 7. IR spectra of the $\text{Fe}_2(\mu\text{-SC}_4\text{H}_3\text{N}_2)_2(\text{NO})_4$ complex (3): experiment minus the background (a) and calculation by the B3LYP (b) and PBE (c) methods.

inphase vibrations of the N(2)–C(3) and N(6)–C(5) bonds, symmetric bending vibrations of the H(C(3)) and H(C(5)) atoms, and C–S stretching vibrations. The symmetric and asymmetric Fe–N vibrations in theoretical spectrum *b* have frequencies of 668 ($m = 18.2$) and 719 cm^{-1} . The latter is characterized by a very minor intensity and is not manifested in the spectrum. Frequencies of 637 ($m = 18.9$) and 432 cm^{-1} correspond to the symmetric and antisymmetric Fe–N–O bending vibrations. According to this calculation, only two bands at 629 and 550 cm^{-1} appear in the region of 486–738 cm^{-1} , where no ligand vibrations are observed (see Fig. 6, *a*). Since in the spectra of complexes **1** and **2** the Fe–N–O bending vibration is higher-intensity, we assign the band at 629 cm^{-1} to the Fe–N–O bending vibration, and the band at 550 cm^{-1} can be ascribed to the Fe–N stretching vibration.

* * *

Thus, calculations by the B3LYP and PBE density functional methods of the structure and electronic

structures of the iron thiolate tetranitrosyl complexes $\text{Fe}_2(\mu\text{-SC}_{6-n}\text{H}_{5-n}\text{N}_n)_2(\text{NO})_4$ ($n = 0, 1, 2$) consistent with the experimental data showed that the spin-paired diamagnetic state of two $\text{Fe}(\text{NO})_2$ units, each having one unpaired electron, is observed in the dimer. The electronic configuration of the $\text{Fe}(\text{NO})_2$ unit with an unpaired electron is formed upon binding of the spin 3/2 of the Fe^{+d^7} center with the oppositely oriented spins 1/2 of two NO groups.

Theoretical approaches provide good description for both the experimental structures of the complexes and their IR spectra. On the one hand, this makes it possible to interpret the IR spectra and, on the other hand, to obtain more detailed new information on the structure of the complexes because of a series of nontrivial peculiarities of the IR spectra of the iron nitrosyl complexes.

A doublet of bands of stretching NO vibrations, whose intensity exceeds those of other bands by an order of magnitude and more, can be distinguished in the spectra of the complexes. The corresponding forces of oscillators of the IR transitions are much higher than the oscillator force for the free NO molecule. It is most likely that this effect appears due to the enhancement of NO polarization in the complex resulting in an increase in the dipole moment of the transition and also to the sensitivity of the donor-acceptor electron density transfer in the Fe–NO fragment to the N–O distance. This specific feature of binding makes it possible to explain the considerable intensity of the NO vibrations in the complexes and a noticeable scatter of the doublet splitting from 15 cm^{-1} for the equivalent NO groups to 55 cm^{-1} for the weakly nonequivalent NO groups with a difference in the N–O and Fe–N distances of about 0.01 Å. Both the batho- and hypsochromic shifts of the vibrational bands of the thiolate ligand in the complexes are reproduced by the theory qualitatively and semiquantitatively. As a whole, the both methods well describe the experimental structure of the spectrum; however, the PBE functional better reflects the absolute positions of the bands, and the B3LYP functional is better in describing their relative intensities.

Experimental

Single crystals of complexes **1–3** were synthesized according to earlier described procedures.^{17–19}

IR spectra were recorded on a Perkin–Elmer 1720X FT-IR spectrometer (KBr pellets, 2 mg of the sample per 300 mg of Br).

This work was financially supported by the Council on Grants of the President of the Russian Federation (Program for State Support of Leading Scientific Schools of Russia, Grant NSh-2150.2006.3).

References

1. G. B. Richter-Addo and P. Legzdins, *Metal Nitrosyls*, Oxford University Press, New York, 1992.
2. M. J. Clarke and J. B. Gaul, *Struct. Bonding (Berlin)*, 1993, **81**, 147.
3. A. R. Butler and D. L. H. Williams, *Chem. Soc. Rev.*, 1993, **22**, 223.
4. R. Ackroyd, C. Kelty, N. Brown, and M. Reed, *Photochem. Photobiol.*, 2001, **74**, 656.
5. R. K. Pandey, *J. Porphyrins Phthalocyanines*, 2000, **4**, 368.
6. P. C. Ford and I. M. Lorkovic, *Chem. Rev.*, 2002, **102**, 993.
7. M. Hoshino, L. E. Laverman, and P. C. Ford, *Coord. Chem. Rev.*, 1999, **187**, 75.
8. C. E. Cooper, *Biochim. Biophys. Acta*, 1999, **1411**, 290.
9. M. D. Wolf, J. V. Parales, D. T. Gibson, and D. J. Lipscomb, *J. Biol. Chem.*, 2001, **276**, 1945.
10. N. A. Sanina and S. M. Aldoshin, *Izv. Akad. Nauk, Ser. Khim.*, 2004, 2326 [*Russ. Chem. Bull., Int. Ed.*, 2004, **53**, 2428].
11. N. A. Sanina, S. M. Aldoshin, T. N. Rudneva, N. I. Golovina, G. V. Shilov, Y. M. Shul'ga, N. S. Ovanesyan, V. N. Ikorskii, and V. I. Ovcharenko, *J. Mol. Struct.*, 2005, **752**, 1110.
12. N. A. Sanina, T. N. Rudneva, S. M. Aldoshin, G. V. Shilov, D. V. Korchagin, Yu. M. Shul'ga, V. M. Martinenko, and N. S. Ovanesyan, *Inorg. Chim. Acta*, 2006, **359**, 570.
13. J. T. Thomas, J. H. Robertson, and E. G. Cox, *Acta Crystallogr.*, 1958, **11**, 599.
14. C. Glidewell, M. E. Harman, M. B. Hursthouse, I. L. Johnson, and M. Motevalli, *J. Chem. Res.*, 1998, **212**, 1676.
15. R. E. Marsh and A. L. Spek, *Acta Crystallogr., Sect. B, Struct. Sci.*, 2001, **57**, 800.
16. Cai Jinhua, Mao Shaoping, Huang Jinling, and Lu Jiayi, *Chinese J. Struct. Chem.*, 1983, **2**, 263.
17. T. B. Rauchfuss and T. D. Weatherill, *Inorg. Chem.*, 1982, **21**, 827.
18. O. A. Rakova, N. A. Sanina, G. V. Shilov, Yu. M. Shul'ga, V. M. Martynenko, N. S. Ovanesyan, and S. M. Aldoshin, *Koord. Khim.*, 2002, **28**, 364 [*Russ. J. Coord. Chem.*, 2002, **28** (Engl. Transl.)].
19. O. A. Rakova, N. A. Sanina, Yu. M. Shul'ga, A. V. Kulikov, and S. M. Aldoshin, *J. Inorg. Biochem.*, 2001, **85**, 390.
20. S. M. Aldoshin, N. A. Sanina, O. A. Rakova, G. V. Shilov, A. V. Kulikov, Yu. M. Shul'ga, and N. S. Ovanesyan, *Izv. Akad. Nauk, Ser. Khim.*, 2003, 1614 [*Russ. Chem. Bull., Int. Ed.*, 2003, **52**, 1702].
21. M. J. Frisch, G. W. Trucks, H. B. Schlegel, G. E. Scuseria, M. A. Robb, J. R. Cheeseman, V. G. Zakrzewski, J. A. Montgomery, Jr., R. E. Stratmann, J. C. Burant, S. Dapprich, J. M. Millam, A. D. Daniels, K. N. Kudin, M. C. Strain, O. Farkas, J. Tomasi, V. Barone, M. Cossi, R. Cammi, B. Mennucci, C. Pomelli, C. Adamo, S. Clifford, J. Ochterski, G. A. Petersson, P. Y. Ayala, Q. Cui, K. Morokuma, D. K. Malick, A. D. Rabuck, K. Raghavachari, J. B. Foresman, J. Cioslowski, J. V. Ortiz, A. G. Baboul, B. B. Stefanov, G. Liu, A. Liashenko, P. Piskorz, I. Komaromi, R. Gomperts, R. L. Martin, D. J. Fox, T. Keith, M. A. Al-Laham, C. Y. Peng, A. Nanayakkara, M. Challacombe, P. M. W. Gill, B. Johnson, W. Chen, M. W. Wong, J. L. Andres, C. Gonzalez, M. Head-Gordon, E. S. Replogle, and J. A. Pople, *GAUSSIAN-98, Revision A.7*, GAUSSIAN, Inc., Pittsburgh (PA), 1998.
22. D. N. Laikov, *Chem. Phys. Lett.*, 1997, **81**, 151.
23. N. A. Sanina, O. A. Rakova, S. M. Aldoshin, G. V. Shilov, Yu. M. Shulga, A. V. Kulikov, and N. S. Ovanesyan, *Mendeleev Commun.*, 2004, **1**, 9.

Received July 17, 2006